Journal of Computing and Electronic Information Management
ISSN: 2413-1660 | Vol. 19, No. 3, 2025

SS-ConvSLSTM: A Study on a Spatiotemporal Temperature Prediction Model for Henan Based on Improved sLSTM

Zhongcai Li*

School of Computer Science and Technology, Henan Polytechnic University, Jiaozuo, China.
* **Corresponding author Email**: 212309010009@home.hpu.edu.cn

Abstract: As a major grain-producing province in China, accurate temperature prediction is crucial for Henan. Addressing the issue of temperature prediction in Henan, this paper proposes a spatiotemporal sequence prediction model named SS-ConvSLSTM, based on an improved sLSTM. The model achieves this through three core innovations: firstly, it employs a 48×48 spatiotemporal data grid for regional holistic prediction, as opposed to traditional single-point forecasting; secondly, it modifies the sLSTM by introducing a convolutional structure to construct ConvSLSTM units, making it suitable for spatiotemporal prediction tasks; and finally, an encoder-decoder network architecture, SS-ConvSLSTM, is built based on the new units to accomplish sequence-to-sequence prediction tasks. Experimental results demonstrate that the model performs excellently in temperature prediction tasks for Henan, achieving significantly higher prediction accuracy compared to traditional baseline models such as LSTM and ConvLSTM, thereby providing a new technological pathway for regional climate prediction.

Keywords: Temperature prediction; MAU; Sequence-to-sequence prediction; LSTM; ConvLSTM.

1. Introduction

Temperature prediction (TP) holds significant importance in modern society, playing a crucial role in various fields such as agriculture, energy management, ecological environment, healthcare, and scientific research. Henan Province, as a major agricultural region and a critical commodity grain production base in China, has relatively low resilience of agricultural production against natural disasters. Therefore, it is essential to strengthen the study of meteorological elements in Henan, understand the patterns of meteorological variations, improve prediction accuracy, and reduce losses caused by disasters.

However, achieving accurate temperature prediction is an extremely challenging task, primarily due to the complexity arising from the multi-dimensional coupling and nonlinear characteristics of spatiotemporal evolution: In the temporal dimension, temperature variations are not simple linear progressions but are driven by the interplay of multiple physical mechanisms. First, multi-scale periodicity and randomness coexist. Although temperature follows distinct diurnal cycles and seasonal trends, it is also influenced by factors such as instantaneous changes in solar radiation intensity, atmospheric circulation fluctuations, and surface heat exchange, resulting in numerous non-stationary signals in the series. Second, the impact of dynamic disturbances: sudden meteorological events (such as cold air intrusions and heatwaves) and micro-scale perturbations (such as instantaneous wind speed changes and cloud cover) introduce strong random fluctuations into temperature series. The superposition of high-frequency noise and low-frequency trends makes it difficult for prediction models to simultaneously ensure long-term stability and accurately capture instantaneous peak changes. In the spatial dimension, temperature distribution exhibits complex spatial autocorrelation and heterogeneity. The evolution of temperature at any single geographical location is not isolated. First, local and regional coupling: the temperature of a given area depends not only on its underlying surface properties (such as vegetation cover, urbanization level, and elevation) but is also influenced by heat advection from adjacent regions. Second, the constraints of complex geographical environments: terrain features (such as mountain barriers to airflow and the moderating effects of water bodies) lead to highly nonlinear heterogeneity in spatial temperature fields, further complicating spatial interpolation and regional prediction. To date, various methods have been proposed for temperature prediction. Existing temperature prediction methods can be broadly categorized into two types: temporal models and spatiotemporal models.

First, traditional models range from statistical inference to shallow machine learning. The core hypothesis of temperature prediction lies in the assumption that the internal dynamic evolution of temperature and its external driving factors (such as meteorological background and topographic features) are implicitly embedded in long-term observational data. By uncovering hidden patterns in historical data, effective estimation of future states can be achieved.

Statistical models: Early research predominantly relied on models such as ARIMA[1][2] and linear regression(LR)[3][4].While these methods are computationally efficient, they are primarily based on linear assumptions and struggle to capture the complex dynamics of atmospheric systems.

Classical machine learning: Subsequently, methods such as Markov models [5][6], genetic algorithms[7][8][9], and support vector machines (SVM)[10][11][12] were introduced. Although these methods excel with small sample datasets, their limitations as "shallow learning" approaches,high dependency on manual feature engineering, and relatively weak ability to extract highly nonlinear and non-stationary temperature fluctuations have constrained prediction accuracy in complex scenarios.

Second, deep learning represents a paradigm shift in

nonlinear feature extraction. The rise of deep learning has brought breakthroughs in temperature prediction. Its core advantage lies in its ability to automatically learn deep nonlinear mappings from vast multi-source data through multi-layered neural network structures, without the need for manual intervention.

Recurrent neural networks (RNN) and their variants: As representatives for processing temporal data, long short-term memory networks (LSTM)[13][14][15] effectively address the gradient vanishing problem in long-sequence training by introducing innovative "gating mechanisms" (input gate, forget gate, output gate). Their variants, such as BiLSTM[16], leverage bidirectional semantic information, and sLSTM[17] further optimizes the memory cell structure, demonstrating excellent performance in capturing long-term trends and short-term fluctuations in temperature.

Feedforward and attention mechanisms: Multilayer perceptrons (MLP)[18][19] provide fundamental fitting capabilities with their simple structures, while Transformer models[20] revolutionize temporal modeling through self-attention mechanisms, enabling parallelized modeling of global dependencies.

Finally, spatiotemporal fusion represents a performance leap by overcoming dimensional limitations. Although the aforementioned models excel in processing one-dimensional time series, temperature is inherently a continuous spatiotemporal field. The temperature at a single site is not only influenced by historical observations but is also closely related to airflow advection and terrain thermal exchange in surrounding geographical areas. To overcome performance bottlenecks, researchers have begun integrating spatial correlations, developing models like ConvLSTM[21][22][23],TGCN[24],3D-CNN[25], MAU[26], PredRNN[27],and D2CL[28]. These methods significantly improve the accuracy of regional temperature predictions by incorporating spatial feature extractors and comprehensively considering the overall spatial effects on target observation points. Despite the notable progress in spatiotemporal fusion models, existing methods still face challenges, particularly in their insufficient ability to learn spatiotemporal features, resulting in suboptimal prediction accuracy.

In summary, temporal models exhibit poor predictive performance due to their neglect of spatiotemporal features, while existing spatiotemporal models lack adequate spatiotemporal feature extraction capabilities, leading to insufficient prediction accuracy. To address this issue, this paper proposes a novel spatiotemporal prediction model, SS-ConvSLSTM, for prediction tasks in Henan. The contributions of this paper are as follows:

1.Design of spatiotemporal data input: 48×48 spatial grid is adopted as input to achieve holistic temperature prediction for the Henan region, fully exploiting spatial correlations.

2.Improvement of the ConvSLSTM unit: 5*5 convolutional kernel is introduced into the traditional sLSTM to enhance spatial feature extraction capabilities, making it suitable for spatiotemporal prediction tasks.

3.Sequence prediction architecture: sequence-to-sequence network structure is designed, where the hidden state output at each step is processed through convolution to serve as the prediction result for the current step and the input for the next step, effectively mitigating error accumulation in multi-step prediction.

The structure of the paper is as follows: Section 2 introduces the basic principles of the model. Section 3 describes the dataset and experimental parameter settings. Section 4 presents, discusses, and analyzes the experimental results of the proposed prediction method. Section 5 summarizes the main conclusions.

2. Methodology

2.1. Problem Definition

Given a historical temperature data sequence $X_{1:T}=\{X_1,X_2,\ldots,X_T\}$ for a 48*48 grid in the Henan region, where $X_t \in R^{48\times48}$ represents the gridded temperature data at time step t. The goal of spatiotemporal prediction is to forecast the temperature sequence for the next Ktime steps, $\hat{X}_{T+1:T+K}=\{\hat{X}_{T+1},\hat{X}_{T+2},\ldots,\hat{X}_{T+K}\}$

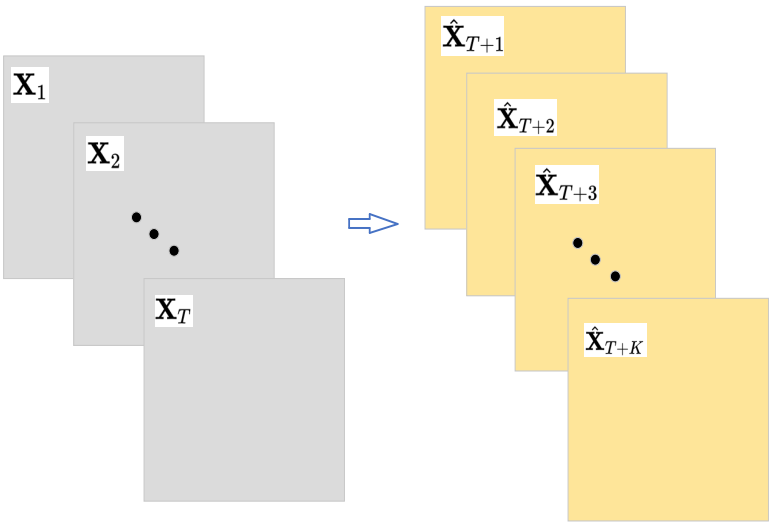

Figure 1. Predicting Future Data Based on Historical Data.

2.2. ConvSLSTM cell

As the cornerstone of spatiotemporal sequence prediction, ConvLSTM achieves synchronous modeling of local spatial features and temporal dynamic evolution by introducing convolutional operators into its gated units. It has achieved remarkable results in fields such as temperature prediction, as illustrated in Equation (1),traditional ConvLSTM employs an input gate i_t, a forget gate f_t, and an output gate o_t, all activated by the sigmoid function σ, while the candidate

memory c_t cell typically uses the tanh function.

$$\begin{aligned} i_t &= \sigma(W_i * x_t + r_i * h_{t-1} + b_i) \\ f_t &= \sigma(W_f * x_t + r_f * h_{t-1} + b_f) \\ \tilde{c}_t &= \tanh(W_c * x_t + r_c * h_{t-1} + b_z) \\ c_t &= f_t \circ c_{t-1} + i_t \circ \tilde{c} \\ o_t &= \sigma(W_o * x_t + r_o * h_{t-1} + b_o) \\ h_t &= o_t \circ \tanh(c_t) \end{aligned} \tag{1}$$

However, its inherent gating mechanism suffers from performance bottlenecks. The Sigmoid activation function strictly confines gating values to the (0, 1) range, leading to exponential attenuation of information when transmitted across time steps, making it difficult to capture ultra-long-term temporal dependencies. Moreover, when processing non-linear signals with extreme fluctuations, traditional saturated activation functions tend to enter gradient saturation regions, limiting their ability to extract complex dynamic features.

$$\begin{aligned} i_t &= \exp(i_t - m_t), & \tilde{i}_t &= W_i * x_t + r_i * h_{t-1} + b_i \\ f_t &= \exp(\tilde{f}_t + m_{t-1} - m_t), & \tilde{f}_t &= \log(\sigma(W_f * x_t + r_f * h_{t-1} + b_f)) \\ c_t &= f_t \circ c_{t-1} + i_t \circ \tilde{c}_t, & \tilde{c}_t &= \tanh(W_c * x_t + r_c * h_{t-1} + b_z) \\ o_t &= \sigma(Wo * x_t + r_o * h_{t-1} + b_o) & & \\ h_t &= o_t \circ \tilde{h}_t, & \tilde{h}_t &= c_t / n_t \\ m_t &= \max(\tilde{f}_t + m_{t-1}, \tilde{i}_t) & & \\ n_t &= f_t \circ n_{t-1} + i_t & & \end{aligned} \tag{2}$$

To address the aforementioned challenges, this paper proposes ConvSLSTM (Convolutional Stabilized LSTM), as expressed in Equation (2). By reconstructing the gating activation mechanism and state update logic, the model significantly enhances its sensitivity to key information and the stability of long-term memory. Unlike the traditional Sigmoid gating, the input gate and forget gate in ConvSLSTM employ the exponential (exp) function. This nonlinear design makes the gating more sensitive to subtle changes in input signals, enabling information amplification and suppression. When the information at the current step exhibits high predictive value, the exp function can generate gain values far greater than 1, thereby achieving significant amplification of information rather than merely allowing it to "pass through." This mechanism breaks away from the "subtractive" logic of traditional models in information retention, endowing the model with the ability to actively enhance key features. To address potential issues of numerical overflow and explosion caused by exponential gating, ConvSLSTM introduces innovative normalization and constraint mechanisms, specifically the normalized state n_t, which dynamically accumulates gating intensity information from all historical time steps. Through automatic scaling of the cell state c_t—leveraging division operations to map exponentially growing information back to a reasonable numerical range—the stability of the hidden state output is ensured. Additionally, the logarithmic constraint state m_t is introduced to further prevent numerical instability during computation. By operating in the logarithmic space, the model effectively monitors and constrains the magnitude of exponential terms, ensuring the convergence of training in deep networks.

Compared to traditional models, ConvSLSTM excels in its self-correcting capability for historical decisions. First, it overcomes the limitation of decay: the exponential gating allows the cell state to undergo "gain accumulation" when necessary, which is crucial for retaining long-term spatiotemporal patterns. Second, it demonstrates dynamic adaptability: through the synergistic action of $n_t$and mm_t, the model achieves a precise balance between amplifying critical information and maintaining numerical stability. Finally, it delivers high-precision fitting: this architecture can more accurately characterize the features of non-stationary and highly volatile meteorological data, providing a more stable foundation for long-sequence, high-difficulty spatiotemporal prediction tasks. The model is illustrated in Figure 2.

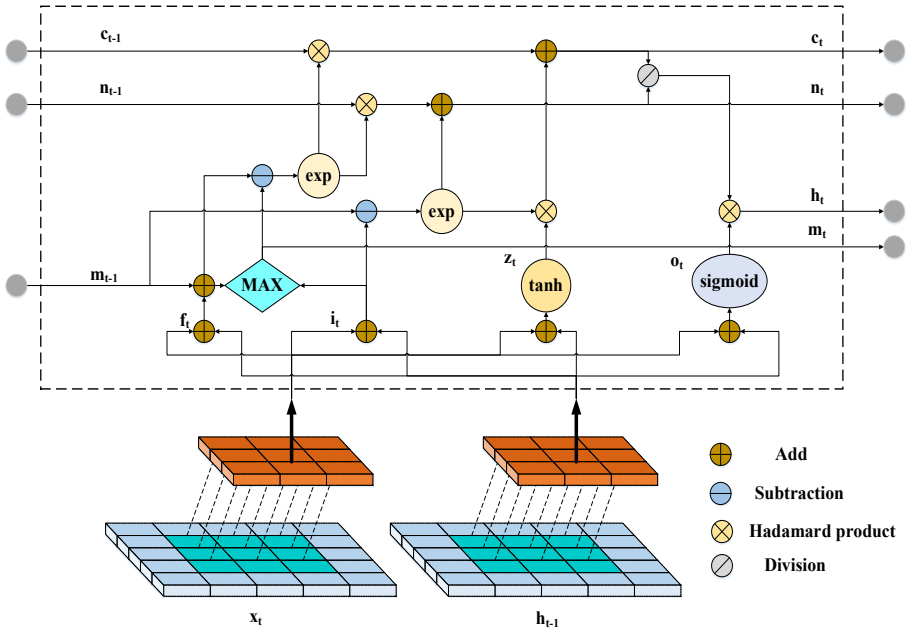

Figure 2. ConvSLSTM cell.

2.3. SS-ConvSLSTM

SS-ConvSLSTM enables sequence-to-sequence prediction, allowing the prediction length to be set arbitrarily based on historical TP information. As shown in Figure 3, assume the number of hidden unit layers is set to 2, the input window length is 2, and the output window length is set to 4.

As shown in Figure 3, it can be seen that we can predict more steps than the length of historical data based on the task requirements. The final convolutional layer is used for feature prediction on the extracted h, where each input step produces an output, but the model only outputs the last few outputs as specified.

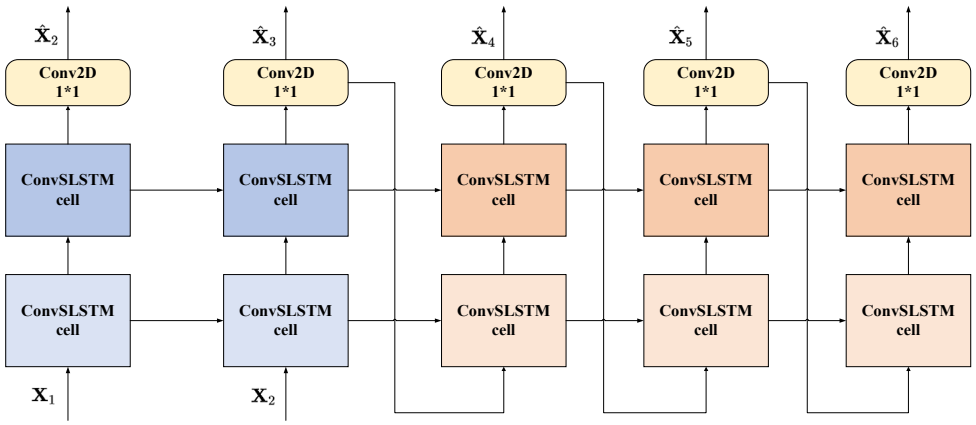

Figure 3. SS-ConvSLSTM Example Model.

3. Experimental Setup

3.1. Study Area

In temperature prediction tasks, the target area is typically divided into equally sized grid cells based on geographic longitude and latitude coordinates. The temperature data within each grid is usually collected by meteorological observation equipment located inside that grid. All grids are arranged along latitude and longitude to form a matrix with dimensions of R*C, representing the regional temperature distribution at a specific time point Ti, where R and C denote the number of grids along the latitude and longitude directions, respectively.

Based on the representation method described above, a chronologically ordered series of temperature matrices can be derived from historical observation data, forming a complete time sequence: T_1, T_2, ..., T_n. The matrix at each time point not only records the spatial temperature distribution at that moment but also exhibits temporal continuity and dependency with matrices from preceding and subsequent time points. Together, they constitute a temperature observation sequence with a spatiotemporal structure, providing a foundational data format for subsequent tasks such as time series prediction, pattern analysis, or spatiotemporal modeling.

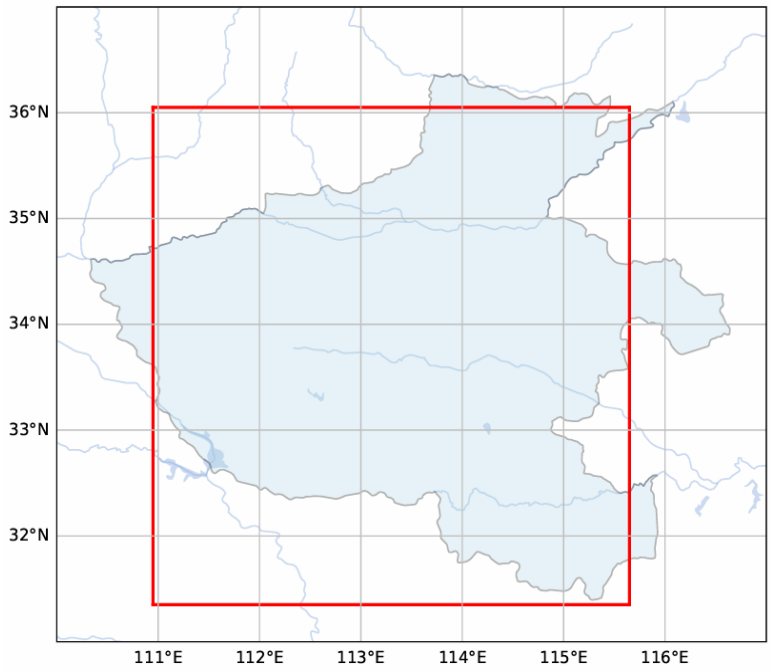

Figure 4. Henan Study Area

Figure 4 illustrates the study area in Henan. The temperature data for Henan is sourced from the China Regional Land Surface Meteorological Elements Driving Dataset provided by the National Tibetan Plateau Scientific Data Center. The matrix data for Henan used in this paper covers the period from 2015 to 2018. The study area spans from 31.35°N to 36.15°N and 110.95°E to 115.75°E, divided into a 48*48 grid. The spatial resolution is 0.1°*0.1°, and the temporal resolution is 3 hours, resulting in a total of 11,688 samples. The data is split into training, validation, and test sets in an 8:1:1 ratio.

3.2. Model Parameter Settings and Model Evaluation Metrics

In this paper, LSTM, sLSTM, MAU, D2CL, and ConvLSTM are used as comparative models. Among them, LSTM, sLSTM, ConvLSTM, and SS-ConvSLSTM are RNN-based architectures. To eliminate the influence of parameters, the number of layers for LSTM, sLSTM, ConvLSTM, and SS-ConvSLSTM is uniformly set to 4.

The input window for all models is set to 8. Since the temporal resolution of the Henan dataset is 3 hours and the spatiotemporal variations are influenced by numerous complex factors, an overly long output window would introduce excessive errors, rendering the results less meaningful. Therefore, the output window is set to 1. The Adam optimizer is used for training, with a learning rate of 0.0001, and an early stopping mechanism is applied with a patience of 10. All experiments are implemented on the Python and PyTorch platforms, utilizing a high-performance server equipped with a 14-core Xeon(R) Gold 6330 CPU and 2 NVIDIA GeForce RTX 3090 GPUs.

To comprehensively evaluate the prediction results of the models, we use Mean Squared Error (MSE) and Mean Absolute Error (MAE) as evaluation metrics. The formulas are as follows:

$$MSE=\frac{1}{n}\sum_{i=1}^{n}(y_i-\hat{y}_i)^2 \quad (3)$$

$$MAE=\frac{1}{n}\sum_{i=1}^{n}|y_i-\hat{y}_i| \quad (4)$$

Mean Squared Error (MSE) measures the average of the squared differences between predicted values and actual observed values, with a value range from zero to positive infinity. In model evaluation, a lower MSE indicates better predictive performance, as it reflects a reduction in the sum of squared prediction errors, meaning the overall deviation between the models output and the true values is smaller. Mean Absolute Error (MAE) calculates the arithmetic average of the absolute differences between predicted values and true values. As a linear scoring metric, MAE assigns equal weight to the error of each sample, providing an intuitive and robust measure of error. It reflects the average magnitude of prediction errors without considering the direction (positive or negative) of the errors. In summary, both MSE and MAE adhere to the evaluation principle of "error minimization": the lower the metric value (closer to zero), the higher the consistency between the models predictions and the true observed values, indicating superior model fitting capability and generalization performance.

4. Experimental Analysis

4.1. The Spatiotemporal Prediction Superiority of SS-ConvSLSTM

Table 1 demonstrates the predictive capabilities of different models on the Henan dataset. SS-ConvSLSTM outperforms all baseline models comprehensively in terms of MSE (Mean Squared Error), while it ranks second-best among most models in terms of MAE (Mean Absolute Error).

The table reveals the significant gains achieved through spatiotemporal fusion. Pure temporal models (LSTM, sLSTM) generally exhibit MSE values above 2.0, while models incorporating spatial feature extraction (D2CL, ConvLSTM, SS-ConvSLSTM) achieve MSE values within the sub-1.8 range. The experimental results strongly confirm the indispensability of spatial correlations in temperature prediction. Relying solely on the temporal evolution patterns (1D) cannot capture critical physical processes such as air mass movement or terrain thermal influences. In contrast, convolution-based models effectively extract these spatially heterogeneous features through convolutional operators, leading to a substantial reduction in prediction errors.

Table 1. Model Prediction Results

Model	MSE	MAE
LSTM	2.350	1.095
sLSTM	2.098	1.029
MAU	2.224	1.111
D2CL	1.793	**0.965**
ConvLSTM	1.773	0.986
SS-ConvSLSTM	**1.715**	0.982

The performance benefits of exponential gating are also evident from the table. In the pure temporal domain, sLSTM achieves an approximately 10.7% reduction in MSE compared to LSTM. In the spatiotemporal domain, SS-ConvSLSTM reduces MSE by about 3.3% compared to ConvLSTM. This validates the effectiveness of the exp function (exponential gating) mentioned earlier. By expanding the gating range from (0, 1) to a larger interval, the model becomes more sensitive to abrupt temperature fluctuations (e.g., sudden cold air intrusions). Unlike standard gating mechanisms, where the sigmoid function saturates and leads to information loss, SS-ConvSLSTM better preserves critical features in long-term memory.

Interestingly, although SS-ConvSLSTM achieves the best MSE performance, D2CL holds a slight advantage in MAE (0.965 vs. 0.982). This may be because MSE is more sensitive to outliers, as it applies a squared penalty that disproportionately amplifies larger prediction errors. SS-ConvSLSTM's clear lead in MSE indicates its greater robustness in handling challenging scenarios such as extreme temperature fluctuations and peak predictions, effectively reducing the occurrence of large errors. The introduced normalized state n_t and logarithmic constraint state m_t in SS-ConvSLSTM successfully mitigate the risk of prediction instability caused by numerical overflow while amplifying important information, thereby ensuring the model's predictive stability.

Compared to MAU and ConvLSTM, the performance advantage of SS-ConvSLSTM stems from its "dynamic correction" capability. MAU may exhibit insufficient generalization when handling extremely complex nonlinear spatial dependencies. ConvLSTM is constrained by its fixed receptive field and gating decay. ConvSLSTM, through its exponentially enhanced gating, essentially simulates an "attention mechanism" that autonomously identifies which historical spatiotemporal slices are more important for future predictions. The "automatic scaling" achieved via division ensures that this enhancement is orderly and stable. Figure 5 illustrates the MAE heatmaps comparing the predicted data of different models with the original data.

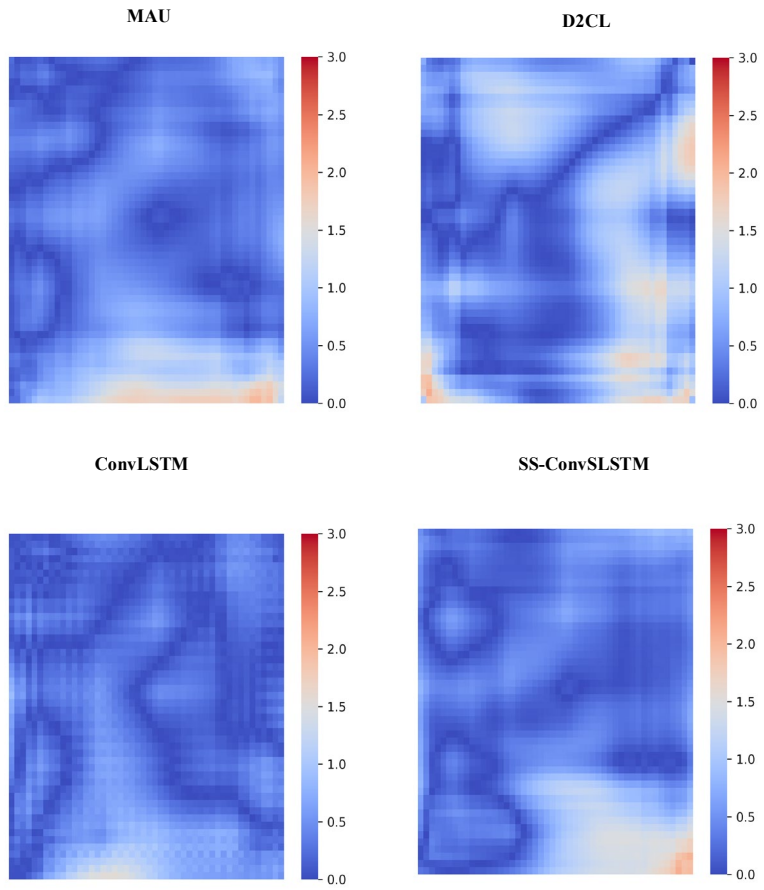

Figure 5. MAE Heatmap of Predictions from Different Models vs. Original Data

4.2. K-value test for convolution kernel

To investigate the impact of convolution kernels of different sizes on temperature prediction performance in Henan, a comparative experiment was conducted. The results are shown in Table 2:

Table 2. Results for Different K-Values

K	MSE	MAE
3	1.735	0.996
5	**1.715**	**0.982**
7	1.721	0.989

As can be seen from the table, when K=3, the error is relatively highest (MSE 1.735). The 3*3 convolution kernel has a small receptive field, causing the model to primarily focus on the target observation point and its immediate neighboring areas. In temperature prediction, this means that while the model captures local thermal variations, it overlooks larger-scale meteorological dynamics, such as the movement of distant cold air masses or the influence of large-scale terrain. Due to insufficient spatial contextual information, the exponential gating in SS-ConvSLSTM cannot fully leverage its advantages in modeling complex spatial dependencies, leading to limited accuracy.

As shown in the table, when K=5, the optimal balance of spatiotemporal features is achieved, with both MSE (1.715) and MAE (0.982) reaching their lowest values. The 5*5 convolution kernel provides a moderate receptive field, effectively covering the key geographical areas influencing the temperature of the target point. It captures mesoscale meteorological features, enabling the exponential gating in SS-ConvSLSTM to identify more representative spatial triggering factors. At this scale, the exp function can precisely amplify spatially meaningful features that are physically relevant without introducing excessive background noise. Experiments confirm that 5*5 is the optimal physical scale for capturing spatiotemporal correlations in the current dataset. As evident from the table, performance peaks at K=5, which represents the vertex (lowest point) of the curve. In meteorological grids, K=5 likely covers the core meteorological radius that affects local temperature variations. For a 48×48 grid, a span of 5 steps is sufficient to encompass a small to medium meteorological scale, aligning with the characteristics of local weather system evolution in atmospheric science.

As indicated in the table, performance declines when K=7. Compared to K=5, a slight deterioration in performance is observed (MSE increases to 1.721). While larger convolution kernels offer a broader global perspective, their drawbacks also emerge. Excessively large kernels may introduce redundant information weakly correlated with the target point or random noise from distant regions. As K increases, the number of parameters grows quadratically, which complicates model training. Given the typically high continuity of temperature fields locally, an excessively large receptive field may blur edge features, making it challenging for the exponential gating in SS-ConvSLSTM to maintain the most precise scaling ratio when processing "overloaded" information.

5. Conclusion

This paper proposes a spatiotemporal prediction model

based on SS-ConvSLSTM to address temperature prediction in the Henan region. Through three core innovations—spatiotemporal data input, ConvSLSTM unit design, and a sequence-to-sequence prediction architecture—the model effectively captures the spatiotemporal dependencies in temperature data. Experimental results on 11,688 data samples from 2015 to 2018 demonstrate that the model outperforms traditional methods across all evaluation metrics, providing an effective solution for regional meteorological prediction.

Future research directions include: further optimizing the network architecture and incorporating attention mechanisms to enhance model interpretability; exploring multivariate prediction by integrating other meteorological factors such as precipitation and humidity; and applying the model to other spatiotemporal prediction tasks, such as traffic flow forecasting and air quality prediction.

References

[1] Masum, M. H., Islam, R., Hossen, M. A. & Akhie, A. A. Time Series Prediction of Rainfall and Temperature Trend using ARIMA Model. Journal of Scientific Research 14, 215–227 (2022).

[2] Amjad, M. et al. Analysis of Temperature Variability, Trends and Prediction in the Karachi Region of Pakistan Using ARIMA Models. Atmosphere 14, (2022).

[3] Menon, S. P., Bharadwaj, R., Shetty, P., Sanu, P. & Nagendra, S. Prediction of temperature using linear regression. in 2017 International Conference on Electrical, Electronics, Communication, Computer, and Optimization Techniques (ICEECCOT) 1–6 (2017). doi:10.1109/ICEECCOT.2017.8284588.

[4] Gupta, I., Mittal, H., Rikhari, D. & Singh, A. K. MLRM: A Multiple Linear Regression based Model for Average Temperature Prediction of A Day. Preprint at https://doi.org/10.48550/arXiv.2203.05835 (2022).

[5] Pang, Z. & Wang, Z. Temperature trend analysis and extreme high temperature prediction based on weighted Markov Model in Lanzhou. Nat Hazards 108, 891–906 (2021).

[6] Johnson, S. D., Battisti, D. S. & Sarachik, E. S. Empirically Derived Markov Models and Prediction of Tropical Pacific Sea Surface Temperature Anomalies. Journal of Climate 13, 3–17 (2000)

[7] Stajkowski, S., Kumar, D., Samui, P., Bonakdari, H. & Gharabaghi, B. Genetic-Algorithm-Optimized Sequential Model for Water Temperature Prediction. Sustainability 12, (2020).

[8] Ren, J., Wang, Z., Pang, Y. & Yuan, Y. Genetic algorithm-assisted an improved AdaBoost double-layer for oil temperature prediction of TBM. Advanced Engineering Informatics 52, 101563 (2022).

[9] Venkadesh, S., Hoogenboom, G., Potter, W. & McClendon, R. A genetic algorithm to refine input data selection for air temperature prediction using artificial neural networks. Applied Soft Computing 13, 2253–2260 (2013).

[10] Quan, Q., Hao, Z., Xifeng, H. & Jingchun, L. Research on water temperature prediction based on improved support vector regression. Neural Comput & Applic 34, 8501–8510 (2022).

[11] Paniagua-Tineo, A. et al. Prediction of daily maximum temperature using a support vector regression algorithm. Renewable Energy 36, 3054–3060 (2011).

[12] Ni, Y. Q., Hua, X. G., Fan, K. Q. & Ko, J. M. Correlating modal properties with temperature using long-term monitoring data and support vector machine technique. Engineering Structures 27, 1762–1773 (2005).

[13] Liu, J. et al. TD-LSTM: Temporal Dependence-Based LSTM Networks for Marine Temperature Prediction. Sensors 18, (2018).

[14] Xiao, C. et al. Short and mid-term sea surface temperature prediction using time-series satellite data and LSTM-AdaBoost combination approach. Remote Sensing of Environment 233, 111358 (2019).

[15] Yang, Y. et al. A CFCC-LSTM Model for Sea Surface Temperature Prediction. IEEE Geoscience and Remote Sensing Letters 15, 207–211 (2018).

[16] Schuster, M. & Paliwal, K. K. Bidirectional recurrent neural networks. IEEE Transactions on Signal Processing 45, 2673–2681 (1997).

[17] Beck, M. et al. xLSTM: Extended Long Short-Term Memory. Preprint at https://doi.org/10.48550/arXiv.2405.04517 (2024).

[18] Mashaly, A. F. & Alazba, A. A. MLP and MLR models for instantaneous thermal efficiency prediction of solar still under hyper-arid environment. Computers and Electronics in Agriculture 122, 146–155 (2016).

[19] Ghritlahre, H. K. & Prasad, R. K. Exergetic performance prediction of solar air heater using MLP, GRNN and RBF models of artificial neural network technique. Journal of Environmental Management 223, 566–575 (2018).

[20] Chen, Q. et al. TemproNet: A transformer-based deep learning model for seawater temperature prediction. Ocean Engineering 293, 116651 (2024).

[21] Shi, X. et al. Convolutional LSTM Network: a machine learning approach for precipitation nowcasting. in Proceedings of the 29th International Conference on Neural Information Processing Systems - Volume 1 vol. 1 802–810 (MIT Press, Cambridge, MA, USA, 2015).

[22] Shi, B. et al. Sea Surface Temperature Prediction Using ConvLSTM-Based Model with Deformable Attention. Remote Sensing 16, (2024).

[23] Huan-tong, G., Zhong-yan, H. U. & Tian-lei, W. ConvLSTM Based Temperature Forecast Modification Model for North China. JTM 28, 405–412 (2022).

[24] Zhao, L. et al. T-GCN: A Temporal Graph Convolutional Network for Traffic Prediction. IEEE Transactions on Intelligent Transportation Systems 21, 3848–3858 (2020).

[25] Higashiyama, K., Fujimoto, Y. & Hayashi, Y. Feature Extraction of NWP Data for Wind Power Forecasting Using 3D-Convolutional Neural Networks. Energy Procedia 155, 350–358 (2018).

[26] Chang, Z. et al. MAU: A Motion-Aware Unit for Video Prediction and Beyond. in Advances in Neural Information Processing Systems vol. 34 26950–26962 (Curran Associates, Inc., 2021).

[27] Wang, Y. et al. PredRNN: A Recurrent Neural Network for Spatiotemporal Predictive Learning. IEEE Transactions on Pattern Analysis and Machine Intelligence 45, 2208–2225 (2023).

[28] Hou, S. et al. D2CL: A Dense Dilated Convolutional LSTM Model for Sea Surface Temperature Prediction. IEEE Journal of Selected Topics in Applied Earth Observations and Remote Sensing 14, 12514–12523 (2021)